

Universal equation of state and pseudogap in the two-dimensional Fermi gas

Marianne Bauer,^{1,*} Meera M. Parish,² and Tilman Enss³

¹*Cavendish Laboratory, Cambridge, CB3 0HE, United Kingdom*

²*London Centre for Nanotechnology, Gordon Street, London, WC1H 0AH, United Kingdom*

³*Institut für Theoretische Physik, Universität Heidelberg, 69120 Heidelberg, Germany*

We determine the thermodynamic properties and the spectral function for a homogeneous two-dimensional Fermi gas in the normal state using the Luttinger-Ward, or self-consistent T-matrix, approach. The density equation of state deviates strongly from that of the ideal Fermi gas even for moderate interactions, and our calculations suggest that temperature has a pronounced effect on the pressure in the crossover from weak to strong coupling, consistent with recent experiments. We also compute the superfluid transition temperature for a finite system in the crossover region. There is a pronounced pseudogap regime above the transition temperature: the spectral function shows a Bogoliubov-like dispersion with back-bending, and the density of states is significantly suppressed near the chemical potential. The contact density at low temperatures increases with interaction and compares well with both experiment and zero-temperature Monte Carlo results.

The formation of fermion pairs and superfluidity of such pairs are distinct but related phenomena: in weak-coupling BCS theory, both are predicted to occur at the same temperature T_c . However, a basic question of many-body physics is how they are related at stronger coupling and in low dimensions, where quantum fluctuations play a large role. While preformed pairs in the normal phase trivially exist in the strong-coupling Bose limit where one has tightly bound dimers, it has been argued that pairing above T_c can also occur in the BCS regime. In this case, one expects a significant suppression of spectral weight at the Fermi surface even above T_c . This so-called pseudogap regime extends up to a crossover temperature $T^* > T_c$, and its spectral and thermodynamic properties deviate strongly from the predictions of Fermi-liquid theory [1]. Recently, pairing and superfluidity have been studied in ultracold atomic gases, which afford accurate control of both the interaction strength and dimensionality, and allow access to the crossover between the BCS and Bose regimes [2]. In these systems, a pseudogap can be detected through the suppression of the spin susceptibility or directly via the spectral function, which is experimentally accessible by ARPES or momentum-resolved rf spectroscopy [3, 4]. The possibility of a pseudogap regime has already been investigated both experimentally and theoretically in three dimensions (3D) [3, 5].

In two-dimensional (2D) Fermi gases, the pseudogap regime is expected to be much more pronounced than in 3D, and a pairing gap has recently been observed experimentally [4]. Here, we compute the spectral function for the homogeneous 2D Fermi gas in the normal phase of the BCS-Bose crossover. We indeed find a strong suppression of the density of states at the Fermi surface above T_c , as shown in Fig. 1. This allows us to map the extent of the pseudogap regime in the temperature-vs-coupling phase diagram (Fig. 4), and we find that it extends further than in 3D [6].

As the binding between fermions increases, the Cooper pairs evolve into a Bose gas of tightly bound molecules.

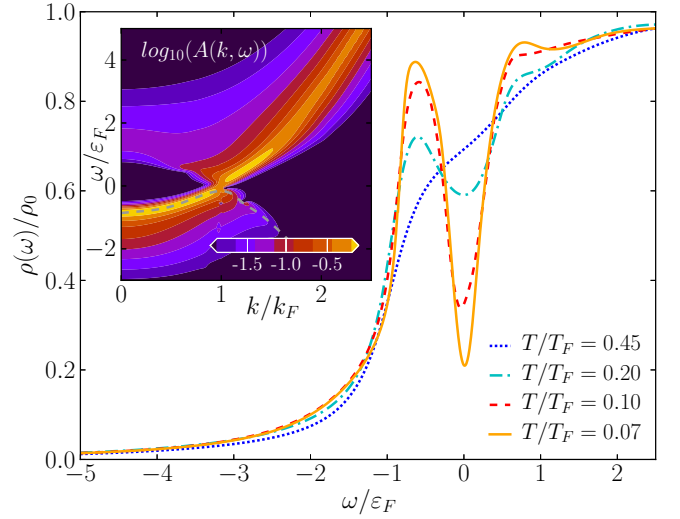


FIG. 1: (Color online) Density of states $\rho(\omega)$, normalised by $\rho_0 = m/2\pi$ for the free Fermi gas, at interaction $\ln(k_F a_{2D}) = 0.8$ for different temperatures: $T = 0.45 T_F$ (top curve at $\omega = 0$) to $T = 0.07 T_F$ (bottom). **Inset:** Spectral function $A(k, \omega)$ for $T = 0.07 T_F$. The grey dashed line marks the maximum in the spectral weight of the bottom band.

Long-range fluctuations in 2D are so strong that they inhibit superfluid long-range order at nonzero temperature. Thus, the 2D Bose gas exhibits a Berezinskii-Kosterlitz-Thouless (BKT) transition at $T_c > 0$ into a quasi-ordered phase with algebraically decaying correlations [7–9]. It is a challenging many-body problem to precisely characterise the crossover between the bosonic BKT and fermionic BCS limits, where the composite nature of the molecules becomes apparent.

In this work, we present the first computation of the finite-temperature density and pressure equation of state in the crossover regime and find a strong renormalisation already for moderate interactions—see Fig. 2. The pressure at low temperatures has very recently been measured

in experiment [10]. We find that the pressure computed at $T \simeq 0.1T_F$ is closer to the experimental data than zero-temperature Monte Carlo calculations [11], offering a resolution of previous discrepancies (Fig. 3). Furthermore, we determine T_c for finite systems (Fig. 4), which is relevant for experiments on quasi-2D atomic gases, in the crossover regime between the known limiting cases [12]. Finally, the contact density agrees well with experiment [13] and shows surprisingly little variation with temperature (Fig. 5).

The dilute, two-component (\uparrow, \downarrow) Fermi gas with short-range interactions is described by the Hamiltonian

$$H = \sum_{\mathbf{k}\sigma} (\varepsilon_{\mathbf{k}} - \mu) c_{\mathbf{k}\sigma}^\dagger c_{\mathbf{k}\sigma} + \frac{g_0}{V} \sum_{\mathbf{k}, \mathbf{k}', \mathbf{q}} c_{\mathbf{k}\uparrow}^\dagger c_{\mathbf{k}'\downarrow}^\dagger c_{\mathbf{k}'+\mathbf{q}\downarrow} c_{\mathbf{k}-\mathbf{q}\uparrow}$$

where $c_{\mathbf{k}\sigma}^\dagger$ creates a fermion with spin σ , momentum \mathbf{k} , and kinetic energy $\varepsilon_{\mathbf{k}} = \hbar^2 \mathbf{k}^2 / 2m$. The chemical potential μ is taken to be the same for both species in a spin-balanced gas. The energy scale is set by the Fermi energy $\varepsilon_F = k_B T_F = \hbar^2 k_F^2 / 2m$ for a total density $n = k_F^2 / 2\pi$. The bare attractive contact interaction g_0 has to be regularised and is expressed in terms of the physical binding energy ε_B of the two-body bound state which is always present in an attractive 2D Fermi gas. We define the 2D scattering length as $a_{2D} = \hbar / \sqrt{m\varepsilon_B}$ and parametrise the interaction strength by $\ln(k_F a_{2D}) = \ln(2\varepsilon_F / \varepsilon_B) / 2$. In the following we set $k_B = 1$, $\hbar = 1$, and write $\beta = 1/k_B T$.

We investigate the behavior of the strongly interacting Fermi gas in the normal state using the Luttinger-Ward, or *self-consistent* T-matrix, approach [14, 15], which goes beyond earlier works [6, 16] by including approximately the interaction between dimers as well as dressed Green's functions. Thermodynamic precision measurements for the unitary Fermi gas in 3D [17] have confirmed the accuracy of this method, both for the value of $T_c/T_F = 0.16(1)$ and the Bertsch parameter $\xi = 0.36(1)$ [15, 17]. Recently, the Luttinger-Ward approach has been extended to study transport properties [18]. The success of this method in three dimensions encourages its application to the homogeneous 2D Fermi gas, which is particularly challenging due to the logarithmic energy dependence of the scattering amplitude.

Within the Luttinger-Ward approach, pairs of dressed fermions with Green's function $G(\mathbf{k}, \omega) = [-\omega + \varepsilon_{\mathbf{k}} - \mu - \Sigma(\mathbf{k}, \omega)]^{-1}$ can form virtual molecules whose dynamics are described by the T matrix $\Gamma(\mathbf{K}, \Omega)$. The fermions can scatter from these molecules, which determines their lifetime and self-energy $\Sigma(\mathbf{k}, \omega)$ (see Supplemental Material [19]). From the self-consistent solution $G(\mathbf{k}, \omega)$ one obtains the spectral function $A(\mathbf{k}, \omega) = \text{Im} G(\mathbf{k}, \omega + i0) / \pi$.

Density of states.—The density of states $\rho(\omega)$ describes at which energies fermionic quasiparticles can be excited, and is computed as the momentum average of the spectral function, $\rho(\omega) = \int d\mathbf{k} A(\mathbf{k}, \omega) / (2\pi)^2$. Figure 1 shows the density of states for an interaction strength of

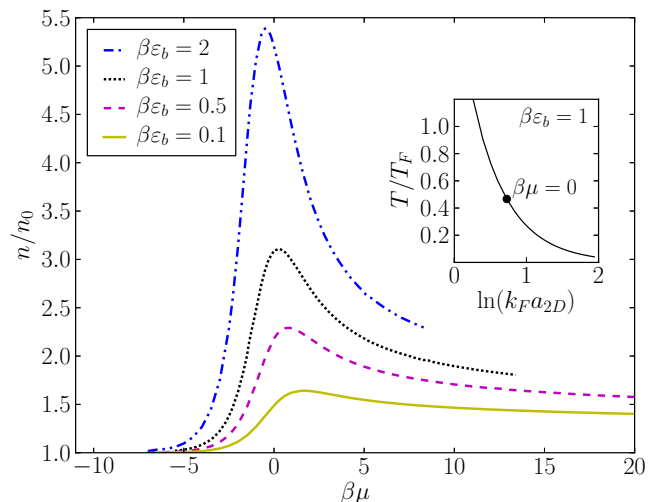


FIG. 2: (Color online) Density n of the 2D Fermi gas vs chemical potential $\beta\mu$, for different interaction strengths $\beta\varepsilon_B$ (see legend). Since the density is normalised by $n_0(\beta\mu)$ for the non-interacting gas, the non-monotonic behavior of n/n_0 reflects the impact of interactions, while the compressibility $\kappa = (\partial n / \partial \mu) / n^2$ is always positive. The inset shows a typical trajectory in T/T_F vs $\ln(k_F a_{2D})$ corresponding to the dotted line of fixed $\beta\varepsilon_B = 1$. Along this line, $\beta\mu$ increases with decreasing T/T_F .

$\ln(k_F a_{2D}) = 0.8$, which is weak enough that there should be a Fermi surface at low temperatures [20]. For decreasing temperature, we see that the density of states is strongly suppressed at the chemical potential, while it increases on either side of the Fermi surface. This marks the pseudogap regime which is part of the normal phase, but with anomalous properties due to the lack of low-energy fermionic excitations. There is no uniquely defined temperature associated with this crossover, so for concreteness we define the pseudogap temperature T^* as the temperature where the density of states at the chemical potential drops by 25% of the value at the left fringe.

The full spectral function $A(\mathbf{k}, \omega)$, shown in the inset of Fig. 1 for a temperature of $T/T_F = 0.07$ slightly above T_c , shows a BCS-like dispersion with a clear reduction of spectral weight near the Fermi energy. While the upper branch has a minimum at a finite wavevector $k \simeq k_F$, the lower branch exhibits “back-bending” towards lower energy for large momenta (cf. Ref. [6]). We note that back-bending alone is not sufficient to define the pseudogap regime and can arise also for other reasons in the occupied spectral function [21]. The two-peak structure of the $k = 0$ spectral function qualitatively agrees with the momentum-resolved RF spectrum measured at $\ln(k_F a_{2D}) = 0.8$ [4], which is the only measurement that may lie within the pseudogap regime [20]. For stronger attraction, the pseudogap regime eventually crosses over into preformed fermion pairs, where the Fermi surface is

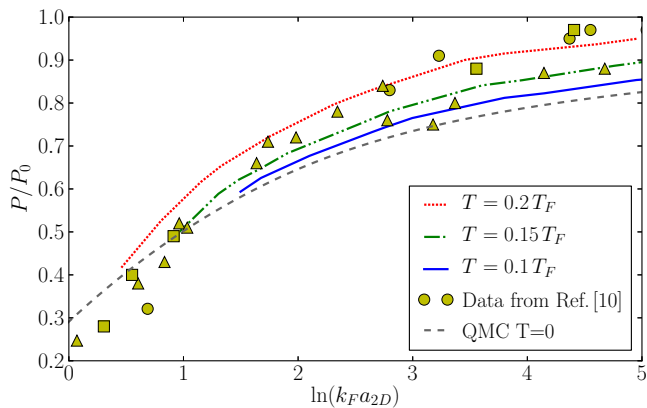


FIG. 3: (Color online) Pressure P vs interaction strength, normalised by the pressure $P_0 = n\varepsilon_F/2$ of an ideal Fermi gas of the same density at $T = 0$. Luttinger-Ward data at temperature $T/T_F = 0.2$ (top, dotted) to $T/T_F = 0.1$ (solid) in comparison with experimental data [10] (symbols) and $T = 0$ Monte Carlo results [11] (dashed).

lost ($\mu < 0$) and the spectral function resembles the one predicted using the virial expansion [20, 22].

Density equation of state.—The total density of both spin components follows from the density of states as $n = 2 \int_{-\infty}^{\infty} d\varepsilon f(\varepsilon)\rho(\varepsilon)$, where $f(\varepsilon)$ is the Fermi distribution. In Fig. 2, we plot the density equation of state $n(\beta\mu, \beta\varepsilon_B)$ as a function of $\beta\mu$ for different values of the interaction parameter $\beta\varepsilon_B$. This manner of plotting the equation of state allows one to make a direct connection with experiments in trapped gases, since the density versus chemical potential at fixed $\beta\varepsilon_B$ can be easily extracted from the measured density profile in a trap [17]. To expose the effects of interactions, we normalise the density n by that of the ideal Fermi gas, $n_0 = 2 \ln(1 + e^{\beta\mu})/\lambda_T^2$, where $\lambda_T = \sqrt{2\pi/mT}$ is the thermal wavelength. In the high-temperature limit where $\beta\mu \rightarrow -\infty$, all properties approach those of an ideal Boltzmann gas. However, with decreasing temperature, we find that n/n_0 eventually exhibits a maximum around $\beta\mu \simeq 0$, implying that interactions are strongest at intermediate temperatures. This is easily understood from the fact that decreasing T/T_F at fixed $\beta\varepsilon_B$ results in an increasing $\ln(k_F a_{2D})$, as shown in the inset of Fig. 2. Thus, we likewise expect the system to approach a weakly interacting gas in the low temperature regime. This behavior is qualitatively different from that observed in 3D [17], and is a direct consequence of the fact that one can have a *density-driven* BCS-Bose crossover in 2D. The curves for large $\beta\varepsilon_B$ are shown up to the critical value $\mu_c(\beta\varepsilon_B)$ where the system is expected to enter the BKT phase.

Pressure.—The pressure is obtained by integrating the density according to the Gibbs-Duhem relation, $P(\mu)_{T,\varepsilon_B} = \int_{-\infty}^{\mu} n(\mu') d\mu'$. Figure 3 shows the Luttinger-Ward data for finite temperatures $T/T_F = 0.2$ (top)

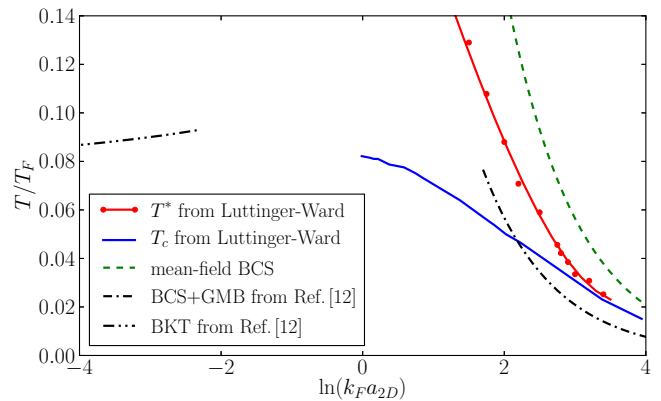


FIG. 4: (Color online) Critical temperature T_c/T_F vs interaction strength $\ln(k_F a_{2D})$. The Luttinger-Ward result for a finite system (blue solid line) in the crossover region $\ln(k_F a_{2D}) \gtrsim 0$ is compared with analytical limits [12]. The red dots marks the crossover temperature T^* to the pseudogap regime for $\ln(k_F a_{2D}) \gtrsim 1$.

to 0.1 (bottom): the pressure decreases from the free Fermi pressure in the BCS limit to the much lower pressure of a dilute Bose gas in the BKT limit. This is a strong coupling effect beyond the mean-field BCS prediction $P = P_0$ at $T = 0$ [10, 11]. As the temperature is lowered, our data approach the $T = 0$ Monte Carlo results [11] (dashed). A recent measurement at low temperatures $T/T_F \simeq 0.04 \dots 0.12$ [10] (symbols) found a deviation from the $T = 0$ pressure in the BCS limit, attributed to mesoscopic effects. We, however, find that the $T/T_F \simeq 0.1$ pressure from the Luttinger-Ward calculation agrees well with experiment in this regime, thus suggesting that the discrepancy is in large part due to the effect of temperature.

Phase diagram of the 2D Fermi gas.—The Berezinskii-Kosterlitz-Thouless (BKT) transition at a finite temperature T_c marks the onset of a nonzero superfluid density ρ_s and algebraically decaying correlations [7, 8]. The jump in ρ_s/n at T_c is universal for a Bose superfluid and becomes exponentially small of order T_c/T_F on the weak-coupling BCS side [23]. The transition temperature is characterised by the Thouless criterion, where the coefficient of the quadratic term in a Ginzburg-Landau action for the pairing field changes sign. In practice, the relevant question is when this transition occurs for a finite system, for instance inside a trapping potential (see Supplemental Material [19]). In our analysis we therefore compute T_c for $N = 500$ particles typical of current experiments [10], as depicted in Fig. 4. We have checked that different values for N lead to small quantitative but not qualitative changes in the T_c curve.

In the weak-coupling BCS limit $\ln(k_F a_{2D}) \gg 1$ [$\varepsilon_B \ll \varepsilon_F$], the mean-field transition temperature is given by $T_c/T_F = (2e^{\gamma_E}/\pi) \exp[-\ln(k_F a_{2D})]$ (dashed

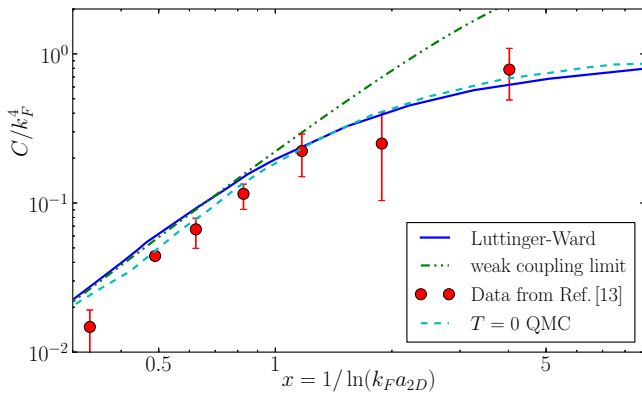


FIG. 5: (Color online) Contact density C vs interaction strength $1/\ln(k_F a_{2D})$ at temperature $T/T_F = 0.27$. We compare our result (blue solid line) with the experimental data at $T/T_F = 0.27$ [13] (red symbols), the weak-coupling result (green dash-dotted line), and Monte Carlo at $T = 0$ [11] (cyan dashed line).

line in Fig. 4), where $\gamma_E \approx 0.5772$ is Euler's constant [24]. Petrov et al. [12] have included Gor'kov–Melik-Barkhudarov corrections and obtained a lower value $T_c/T_F = (2e^{\gamma_E}/\pi e) \exp[-\ln(k_F a_{2D})]$ (dash-dotted line). On the BKT side for strong binding $\varepsilon_B \gg \varepsilon_F$, the Thouless criterion fixes $\mu_c = -\varepsilon_B/2$ and the number equation determines T_c [25]. A more elaborate analysis using Monte Carlo data for the weakly interacting Bose gas in 2D [8] yields a BKT temperature of $T_c/T_F \lesssim 0.12$ for $\ln(k_F a_{2D}) < 0$ [12], which decreases for even stronger binding (left dashed curve in Fig. 4). This limiting behaviour implies the existence of a maximum T_c in the crossover region (cf. Ref. [26]), but does not determine its value or the precise crossover behaviour.

The Luttinger-Ward result for T_c grows monotonically from the BCS limit towards strong coupling $\ln(k_F a_{2D}) \approx 0$: it suggests a maximum T_c at negative $\ln(k_F a_{2D})$, which is unlikely to exceed $T_c/T_F \lesssim 0.1$. This is consistent with experiments which did not observe signatures of superfluidity down to $T/T_F = 0.27$ [4], but is considerably lower than a recent calculation for a harmonically trapped gas [6].

The red dots in the phase diagram in Fig. 4 mark the crossover temperature to the pseudogap regime T^* , where the density of states $\rho(\omega)$ at the chemical potential drops by 25% of the value at the left fringe. In the weak coupling BCS limit, T^* approaches T_c since pairing and condensation occur simultaneously, and both T_c and T^* tend towards the dashed weak-coupling result. The large pseudogap regime at strong binding leads to clear signatures in the spin susceptibility and spectral properties well within reach of current experiments.

Contact density.—The contact density C [27] characterises the probability of finding particles of opposite spin

close to each other [28]. It determines the *universal* high-energy properties of a quantum gas with contact interactions, e.g., the momentum distribution function $n_k \rightarrow C/k^4$ at large momenta. The contact density is related to the variation of the pressure with scattering length by the adiabatic theorem [20, 29],

$$C = -2\pi m \left. \frac{dP}{d \ln a_{2D}} \right|_{\mu, T, V}.$$

Using the weak-coupling expansion of the ground state energy in $x = 1/\ln(k_F a_{2D})$ [30] one obtains at $T = 0$: $C = k_F^4 [x^2 - (3/2 - 2 \ln 2)x^3]/4$. In the normal state the contact density corresponds to the total density of dimers [31].

In Fig. 5 we show our result for the contact (solid line) at $T = 0.27 T_F$ and compare with the experimental data at the same temperature from Fröhlich et al. [13], as well as with the weak-coupling estimate above. Remarkably, our calculation in this low-temperature region is very close to the $T = 0$ Monte Carlo result [11] (dashed line), showing that the contact has only a weak temperature dependence. Note, further, that while one generally expects the contact to decrease with increasing temperature, our result for larger $\ln(k_F a_{2D})$ is higher than the contact at $T = 0$ from Monte Carlo, thus suggesting that C is a non-monotonic function of T , similarly to 3D [32].

In conclusion, we have presented results for the density and pressure equation of state which shed light on a recent pressure measurement [10]. The values for the transition temperature T_c and the pseudogap crossover temperature T^* in the phase diagram reveal a large pseudogap regime; its effect on the spectral function and low-energy density of states are accessible and relevant for current experiments using momentum-resolved rf spectroscopy [4]. We find that the contact depends only weakly on temperature, providing a robust interaction gauge. It will be worthwhile to extend the Luttinger-Ward technique into the low-temperature BKT phase, which is characterised by binding of vortex-antivortex pairs, and study the signatures of the superfluid phase for a trapped 2D Fermi gas. The BKT transition itself is revealed by a jump in the sound velocities [33].

We thank Wilhelm Zwerger for suggesting the problem, valuable discussions and careful reading of the manuscript. We acknowledge discussions with Marcus Barth, Stefan Baur, Gianluca Bertaina, Rudolf Haussmann, Selim Jochim, Michael Köhl, Jesper Levinsen, Vudtiwat Ngampruetikorn, Richard Schmidt and Andrey Turlapov. MB thanks the Gates Cambridge Trust for financial support. MMP acknowledges support from the EPSRC under Grant No. EP/H00369X/2.

* Electronic address: msb50@cam.ac.uk

- [1] M. Randeria, Proceedings of the International School of Physics “Enrico Fermi” Course CXXXVI on High Temperature Superconductors, pp. 53–75 (IOS Press, Amsterdam, 1998); V. M. Loktev, R. M. Quick, and S. G. Sharapov, Phys. Rep. **349**, 1 (2001).
- [2] I. Bloch, J. Dalibard, and W. Zwerger, Rev. Mod. Phys. **80**, 885 (2008); W. Zwerger, ed., *The BCS–BEC Crossover and the Unitary Fermi Gas*, Lecture Notes in Physics, Vol. 836 (Springer, Berlin, 2012).
- [3] J. T. Stewart, J. P. Gaebler, and D. S. Jin, Nature **454**, 744 (2008); J. P. Gaebler, J. T. Stewart, T. E. Drake, D. S. Jin, A. Perali, P. Pieri, and G. C. Strinati, Nature Physics **6**, 569 (2010).
- [4] M. Feld, B. Fröhlich, E. Vogt, M. Koschorreck, and M. Köhl, Nature **480**, 75 (2011).
- [5] Q. Chen, J. Stajic, S. N. Tan, and K. Levin, Phys. Rep. **412**, 1 (2005); Y. He, Q. Chen, and K. Levin, Phys. Rev. A **72**, 011602 (2005); Q. Chen, C. A. Regal, M. Greiner, D. S. Jin, and K. Levin, Phys. Rev. A **73**, 041601 (2006); A. Perali, F. Palestini, P. Pieri, G. C. Strinati, J. T. Stewart, J. P. Gaebler, T. E. Drake, and D. S. Jin, Phys. Rev. Lett. **106**, 060402 (2011).
- [6] R. Watanabe, S. Tsuchiya, and Y. Ohashi, Phys. Rev. A **88**, 013637 (2013).
- [7] D. S. Fisher and P. C. Hohenberg, Phys. Rev. B **37**, 4936 (1988); Z. Hadzibabic, P. Krüger, M. Cheneau, B. Batteletier, and J. Dalibard, Nature **441**, 1118 (2006).
- [8] N. Prokof’ev and B. Svistunov, Phys. Rev. A **66**, 043608 (2002).
- [9] M. Holzmann, G. Baym, J.-P. Blaizot, and F. Laloë, Proc. Natl Acad. Sci. USA **104**, 1476 (2007).
- [10] V. Makhalov, K. Martiyanov, and A. Turlapov, Phys. Rev. Lett. **112**, 045301 (2014).
- [11] G. Bertaina and S. Giorgini, Phys. Rev. Lett. **106**, 110403 (2011).
- [12] D. S. Petrov, M. A. Baranov, and G. V. Shlyapnikov, Phys. Rev. A **67**, 031601 (2003).
- [13] B. Fröhlich, M. Feld, E. Vogt, M. Koschorreck, M. Köhl, C. Berthod, and T. Giamarchi, Phys. Rev. Lett. **109**, 130403 (2012).
- [14] R. Haussmann, Z. Phys. B **91**, 291 (1993); R. Haussmann, Phys. Rev. B **49**, 12975 (1994).
- [15] R. Haussmann, W. Rantner, S. Cerrito, and W. Zwerger, Phys. Rev. A **75**, 023610 (2007).
- [16] P. Nozières and S. Schmitt-Rink, J. Low Temp. Phys. **59**, 195 (1985); S. Schmitt-Rink, C. M. Varma, and A. E. Ruckenstein, Phys. Rev. Lett. **63**, 445 (1989).
- [17] M. J. H. Ku, A. T. Sommer, L. W. Cheuk, and M. W. Zwierlein, Science **335**, 563 (2012).
- [18] T. Enss, R. Haussmann, and W. Zwerger, Ann. Phys. (NY) **326**, 770 (2011); T. Enss and R. Haussmann, Phys. Rev. Lett. **109**, 195303 (2012).
- [19] See Supplemental Material at URL for a description of the Luttinger-Ward approach, alternative definitions of a_{2D} , and the Thouless criterion for finite systems.
- [20] V. Ngampruetikorn, J. Levinsen, and M. M. Parish, Phys. Rev. Lett. **111**, 265301 (2013).
- [21] W. Schneider and M. Randeria, Phys. Rev. A **81**, 021601(R) (2010).
- [22] M. Barth and J. Hofmann, Phys. Rev. A **89**, 013614 (2014).
- [23] S. Stintzing and W. Zwerger, Phys. Rev. B **56**, 9004 (1997).
- [24] K. Miyake, Progr. Theor. Phys. **69**, 1794 (1983).
- [25] C. A. R. Sá de Melo, M. Randeria, and J. R. Engelbrecht, Phys. Rev. Lett. **71**, 3202 (1993).
- [26] M. Drechsler and W. Zwerger, Ann. Phys. (Berlin) **1**, 15 (1992).
- [27] S. Tan, Ann. of Phys. **323**, 2952 (2008); C. Langmack, M. Barth, W. Zwerger, and E. Braaten, Phys. Rev. Lett. **108**, 060402 (2012).
- [28] E. Braaten and L. Platter, Phys. Rev. Lett. **100**, 205301 (2008).
- [29] S. Tan, Ann. Phys. (NY) **323**, 2971 (2008); F. Werner and Y. Castin, Phys. Rev. A **86**, 013626 (2012).
- [30] P. Bloom, Phys. Rev. B **12**, 125 (1975); J. R. Engelbrecht, M. Randeria, and L. Zhang, Phys. Rev. B **45**, 10135 (1992).
- [31] R. Haussmann, M. Punk, and W. Zwerger, Phys. Rev. A **80**, 063612 (2009); R. Combescot, F. Alzetto, and X. Leyronas, Phys. Rev. A **79**, 053640 (2009); Y. Nishida, Phys. Rev. A **85**, 053643 (2012).
- [32] Z. Yu, G. M. Bruun, and G. Baym, Phys. Rev. A **80**, 023615 (2009).
- [33] T. Ozawa and S. Stringari, Phys. Rev. Lett. **112**, 025302 (2014).
- [34] J. R. Engelbrecht and M. Randeria, Phys. Rev. Lett. **65**, 1032 (1990).
- [35] M. Randeria, J.-M. Duan, and L.-Y. Shieh, Phys. Rev. Lett. **62**, 981 (1989).

Supplemental Material: “Universal equation of state and pseudogap in the two-dimensional Fermi gas”
by M. Bauer, M. M. Parish, and T. Enss

Luttinger-Ward approach

The fully dressed fermionic propagator $G(\mathbf{k}, i\omega)$ is calculated from the bare propagator $G_0(\mathbf{k}, i\omega) = [-i\omega + \varepsilon_{\mathbf{k}} - \mu]^{-1}$ via the Dyson equation

$$G^{-1}(\mathbf{k}, i\omega) = G_0^{-1}(\mathbf{k}, i\omega) - \Sigma(\mathbf{k}, i\omega), \quad (1)$$

where $\omega = (2n+1)\pi T$ are fermionic Matsubara frequencies, and $\Sigma(\mathbf{k}, i\omega)$ is the self-energy which captures the interaction effects.

Dilute Fermi gases are well described in the ladder, or T-matrix, approximation. The bosonic vertex function is then given by

$$\Gamma(\mathbf{K}, i\Omega) = [g_0^{-1}(\Lambda) + \chi(\mathbf{K}, i\Omega)]^{-1} \quad (2)$$

in terms of the bare coupling $g_0(\Lambda)$, which depends on the UV momentum cutoff Λ (see below), and the pair propagator

$$\chi(\mathbf{K}, i\Omega) = \int \frac{d\mathbf{k}}{(2\pi)^2} \frac{1}{\beta} \sum_{\omega} G(\mathbf{k}, i\omega) G(\mathbf{K} - \mathbf{k}, i\Omega - i\omega) \quad (3)$$

for bosonic Matsubara frequencies $\Omega = 2n\pi T$. In the ladder approximation the bosonic vertex function is equivalent to the T matrix, which describes the propagation of bound fermion pairs, or dimers, via dressed fermion-fermion excitations. Finally, the fermionic self-energy describes how fermions scatter off (virtual) dimers,

$$\Sigma(\mathbf{k}, i\omega) = \int \frac{d\mathbf{K}}{(2\pi)^2} \frac{1}{\beta} \sum_{\Omega} G(\mathbf{K} - \mathbf{k}, i\Omega - i\omega) \Gamma(\mathbf{K}, i\Omega). \quad (4)$$

The pair propagator χ has a logarithmic ultraviolet divergence [34]; this is regularised by expressing the bare coupling $g_0(\Lambda)$ in Eq. (2) in terms of the physical binding energy ε_B of the two-body bound state which is always present in an attractive 2D Fermi gas,

$$\frac{1}{g_0(\Lambda)} = - \int^{\Lambda} \frac{d\mathbf{k}}{(2\pi)^2} \frac{1}{2\varepsilon_{\mathbf{k}} + \varepsilon_B}. \quad (5)$$

Note that the existence of a bound state is both necessary and sufficient for pairing in 2D [35].

Equations (1)–(4) constitute a set of coupled integral equations. The convolution integrals (3) and (4) are computed in Fourier space (\mathbf{x}, τ) on a logarithmic grid of

400×400 grid points [14] to account for the logarithmically slow decay of the T matrix in 2D. The integral equations are solved by iteration, and once convergence is reached one obtains the self-consistent fermion Green’s function $G(\mathbf{k}, i\omega)$ and the T matrix $\Gamma(\mathbf{K}, i\Omega)$, respectively. $G(\mathbf{k}, i\omega)$ is analytically continued to real frequencies $i\omega \rightarrow \omega + i0$ using Padé approximants to determine the spectral function $A(\mathbf{k}, \omega) = \text{Im} G(\mathbf{k}, \omega + i0)/\pi$.

In the Luttinger-Ward approach, the density is most conveniently obtained from the Green’s function in Fourier space as $n = -2G(\mathbf{x} = 0, \tau = -0)$ without the need for analytical continuation. Similarly, in the normal state, the contact density corresponds to the total density of dimers [31] and can be expressed in terms of the self-consistent T matrix as $C = -m^2\Gamma(\mathbf{x} = 0, \tau = -0)$.

Definition of the 2D scattering length

The interaction strength in a purely 2D system is characterized by the physical binding energy ε_B , see Eq. (5), but different definitions of the scattering length a_{2D} are used in the literature. We follow the convention that $\varepsilon_B = \hbar^2/ma_{2D}^2$, and hence $a_{2D} = \hbar/\sqrt{m\varepsilon_B}$ [4]. Alternatively, one may use $\varepsilon_B = 4\hbar^2/ma_{2D}^2 e^{2\gamma_E}$, and consequently $a_{2D}^{\text{alt}} = (2/e^{\gamma_E})\hbar/\sqrt{m\varepsilon_B} = (2/e^{\gamma_E})a_{2D}$, see e.g. [10, 11]. In a quasi-2D system realized by a harmonic confinement in the third direction, as is common for ultracold atomic gases, ε_B is related to the confinement length ℓ_z and the 3D scattering length a , which can be tuned by a magnetic Feshbach resonance [2, 12]. Ref. [10] argues that the correct quasi-2D scattering length in the Bose limit is obtained by matching the scattering amplitudes of the pure and quasi-2D systems. The interaction parameter $a_{2D}^{\text{alt}}\sqrt{n_2}$ used in that work is related to our definition by $k_F a_{2D} = \sqrt{\pi} e^{\gamma_E} a_{2D}^{\text{alt}}\sqrt{n_2}$ for a single-spin density $n_2 = k_F^2/4\pi$.

Thouless criterion for finite systems

The transition temperature T_c is characterised by the Thouless criterion, $\text{Re} \Gamma^{-1}(\mathbf{K} = 0, i\Omega = 0) = 0$ [14]. The T matrix is proportional to the Green’s function G_{bos} of a dilute Bose gas as $\Gamma^{-1}(\mathbf{K}, i\Omega) = (m/4\pi\varepsilon_B)G_{\text{bos}}^{-1}(\mathbf{K}, i\Omega)$ in the BKT limit [14], and the Bose Green’s function for an N -particle system with coherence length ζ approaches $G_{\text{bos}}^{-1}(\mathbf{K} = 0, i\Omega = 0) = -1/2m\zeta^2 \simeq -T/N$ [9]. In our analysis we therefore consider the Thouless criterion $\text{Re} \Gamma^{-1}(\mathbf{K} = 0, i\Omega = 0) = -m/(4\pi\beta\varepsilon_B N)$ for $N = 500$ particles typical of current experiments [10].